Short communication

Thermal decomposition kinetics of the Pb$_{0.25}$Ba$_{0.75}$(TNR)·H$_2$O complex

Rongzu Hu[a,b,*], Sanping Chen[b], Shengli Gao[b], Fengqi Zhao[a], Yang Luo[a], Hongxu Gao[a], Qizhen Shi[b], Hongan Zhao[b], Pu Yao[c], Jing Li[c]

[a] Xi'an Modern Chemistry Research Institute, Xi'an 710065, China
[b] Shaanxi Key Laboratory of Physico-Inorganic Chemistry and Department of Chemistry, Northwest University, Xi'an 710069, China
[c] Shaanxi Applied Physical Chemistry Research Institute, Xi'an, China

Abstract

Studies of the non-isothermal decomposition of Pb$_{0.25}$Ba$_{0.75}$(TNR)·H$_2$O (TNR = 2,4,6-trinitro-1,3-dihydroxy-benzene) were carried out by means of TG–DTA, DSC and IR techniques. The thermal decomposition mechanism and the associated kinetics have been investigated. The kinetic parameters were obtained from the analysis of the DSC curves by integral and differential methods. The most probable kinetic model function of the dehydration reaction of Pb$_{0.25}$Ba$_{0.75}$(TNR)·H$_2$O were suggested by comparison of the kinetic parameters.
© 2004 Published by Elsevier B.V.

Keywords: Pb$_{0.25}$Ba$_{0.75}$(TNR)·H$_2$O complex; DSC; Non-isothermal kinetics; TG–DTA; Thermal decomposition

1. Introduction

The Pb$_{0.25}$Ba$_{0.75}$(TNR)·H$_2$O (TNR = 2,4,6-trinitro-1,3-dihydroxy-benzene) complex has good detonating properties and is sensitive to flame. It could be used as initiating agent, igniter powder and delay powder. The crystal structure [1] of barium 2,4,6-trinitro-1,3-dihydroxybenzene and lead 2,4,6-trinitro-1,3-dihydroxybenzene complex and the thermal behavior [2] of Pb$_{0.25}$Ba$_{0.75}$(TNR)·H$_2$O have been reported. In the present work, we report its kinetic parameters and mechanism of thermal decomposition reaction studied with TG–DTA, IR and DSC techniques. This is quite useful in the evaluation of its thermal stability under non-isothermal condition and in the study of its thermal changes at high temperature.

2. Experimental

2.1. Material

The single crystal of Pb$_{0.25}$Ba$_{0.75}$(TNR)·H$_2$O used in this work was prepared by Shaanxi Applied Physical Chemistry Research Institute according to a reported method [3]. The single crystal with dimensions of 0.3 mm × 0.3 mm × 0.1 mm was selected for the experiment.

2.2. Equipment and conditions

TG–DTA and DSC curves under static air condition were obtained using a LCT-1 thermal analyzer (Beijing Optical Instrument Factory, China), and a CDR-1 differential scanning calorimeter (Shanghai Tianping Instrument Factory, China), respectively. The conditions of TG–DTA were as follows: sample mass, about 1 mg; heating rate, 10 °C min^{-1}; measurement range: 2 mg (TG), 25 μV (DTA) and 5 mV (temperature). The conditions of the DSC analyses were: sample mass, about 0.5 mg; heating rates, 2, 5, 10 and 20 °C min^{-1};

* Corresponding author. Fax: +86 29 88220423.
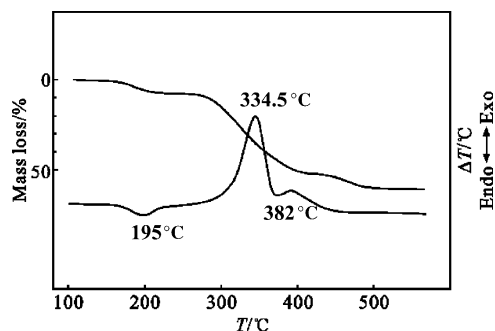 E-mail address: hurongzu@public.xa.sn.cn (R. Hu).

Fig. 1. TG and DTA curves for the title complex in static air at a heating rate of $10\,°C\,min^{-1}$.

Fig. 2. DSC curve for the title complex in static air at a heating rate of $10\,°C\,min^{-1}$.

calorimetric range, ± 20.92 and $\pm 41.84\,mJ\,s^{-1}$; reference sample, α-Al_2O_3. Heating rate is calculated according to the actual rate of temperature rise from $50\,°C$ to the temperature at the end of decomposition. The resolution of temperature was $0.25\,°C$.

The thermal decomposition process of the complex under the condition of flowing N_2 gas was studied on a TA2100 TG–DTA instrument (TA Co., USA) and a type of 910-DSC instrument in TA2000 system (TA, USA). The conditions of TG–DTA were as follows: sample mass, about $0.5\,mg$; heating rate, $10\,°C\,min^{-1}$; flowing rate of N_2 gas, $120\,cm^3\,min^{-1}$; reference sample, α-Al_2O_3. The conditions of DSC were as follows: sample mass, about $1\,mg$; heating rates, 2, 5, 10 and $15\,°C\,min^{-1}$; atmosphere, flowing rate of N_2 gas, $60\,cm^3\,min^{-1}$; reference sample, α-Al_2O_3. All the experiments in both atmospheres were carried out using Al-crucibles. DSC were obtained under the same conditions overlapped with each other, indicating that the reproductively of tests was satisfactory.

The infrared spectra of the complex before and after thermal decomposition were recorded using KBr disc technique on a Perkin-Elmer Model 180 IR spectrophotometer.

3. Results and discussion

3.1. The thermal decomposition mechanism of the complex under static air conditions

The TG–DTA and DSC curves of the complex under static air conditions are shown in Figs. 1 and 2, respectively. The results show that there are one endothermic and two exothermic processes at temperatures higher than $150\,°C$. In Table 1, the initial and final temperatures of the thermal decomposition processes and the mass losses observed between these temperatures in TG curve are given. The enthalpy of the dehydration reaction (ΔH_{deh}) and enthalpy of the major exothermic decomposition reaction (ΔH_{dec}) are also listed. The characteristic absorption peaks of the title complex and the residue formed after each DSC peak, and their tentative assignments are listed in Table 2. The results show that the endothermic process attributed to the loss of
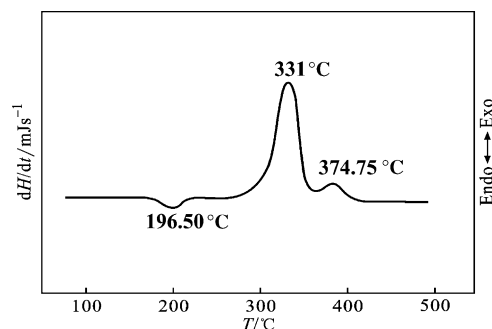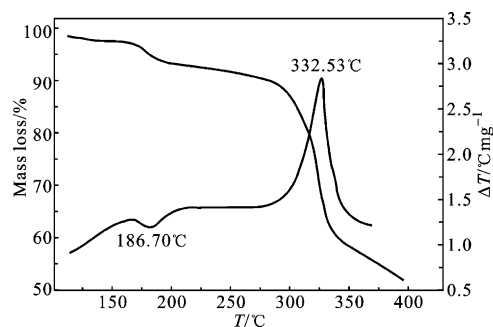

Fig. 3. TG–DTA curve for the complex at a heating rate of $10\,°C\,min^{-1}$ and a flowing rate of N_2 gas of $120\,cm^3\,min^{-1}$.

one water molecule. Further decomposition of the dehydrated complex, $Pb_{0.25}Ba_{0.75}(TNR)$ would occur on heating. The characteristic absorption peaks of the residue formed after the first exothermic peak at 3400, 2160, 1600, 1400, 870 and $770\,cm^{-1}$, indicating that the decomposition residue for this stage is a non-crystalline inorganic mixture [4]. The characteristic absorption peaks of the residue formed after the second exothermic peak at 1430, 1050, 855 and $690\,cm^{-1}$ are assigned to $BaCO_3$. The formation of $0.75BaCO_3$, $0.25PbO$ and carbon from the original sample should be accomplished with a theoretical overall mass loss of 48.06%. This value is in agreement with the experimental value of 49.07%.
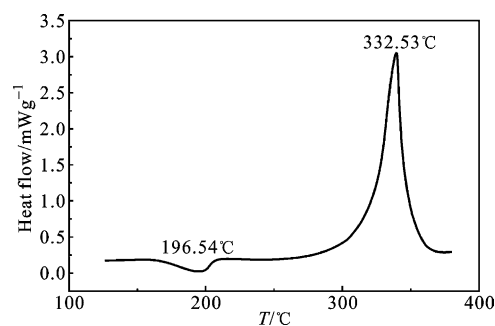

Fig. 4. DSC curve for the complex at a heating rate of $10\,°C\,min^{-1}$ and a flowing rate of N_2 gas of $60\,cm^3\,min^{-1}$.

Table 1
The thermal decomposition data of $Pb_{0.25}Ba_{0.75}(TNR)\cdot H_2O$ obtained by TG and DSC at a heating rate of $10\,°C\,min^{-1}$

Decomposition stage	TG temperature range (°C)	Mass loss (%), observed (calculated)	ΔH_{deh} (J g^{-1})[a]	ΔH_{dec} (J g^{-1})[b]
$Pb_{0.25}Ba_{0.75}(TNR)\cdot H_2O \xrightarrow{-H_2O} Pb_{0.25}Ba_{0.75}(TNR)$	173–229	4.40 (4.33)	177.26 ± 1.27[c]	
$\xrightarrow{-3NO_2}$ non-crystalline inorganic compound	288–359	33.2 (33.2)		2450.0 ± 61.6[d]
$\rightarrow 0.75BaCO_3 + 0.25PbO + C$	359–500	11.83 (10.53)		

[a] Enthalpy of the dehydration reaction.
[b] Enthalpy of the major exothermic decomposition reaction.
[c] Average of seven experiments.
[d] Average of five experiments.

Table 2
IR data of $Pb_{0.25}Ba_{0.75}(TNR)\cdot H_2O$ and its decomposition products

Temperature (°C)	IR data (cm^{-1})	Tentative assignments
RT	3460; 1630	H_2O
	1570; 1550; 1520; 1310	Ar-NO$_2$
	3100; 1470; 1415; 780; 700	Ar
	1220	Ar-O
229	3060; 1470; 1410; 790; 690	Ar
	1550; 1510; 1320	Ar-NO$_2$
	1200	Ar-O
359	3400 (s, b); 2160 (s); 1600(s, b)	Non-crystalline inorganic compound [4]
	1400 (s, b); 870; 770 (w)	
528	1430 (s, b); 1050 (w); 855 (m); 690 (m)	BaCO$_3$

s: strong, w: weak, m: medium, b: broad.

On the bases of these obtained results, the thermal decomposition mechanism of the complex could be shown as

$$Pb_{0.25}Ba_{0.75}(TNR)\cdot H_2O \xrightarrow[173-229\,°C]{-H_2O} Pb_{0.25}Ba_{0.75}(TNR)$$

$$\xrightarrow[288-359\,°C]{-3NO_2} \text{non-crystalline inorganic mixture}$$

$$\xrightarrow[359-528\,°C]{} 0.75BaCo_3 + 0.25PbO + C$$

3.2. The thermal decomposition behavior of the complex in flowing N_2 gas

The typical TG–DTA and DSC curves for the thermal decomposition of the complex under the condition of flowing N_2 gas are shown in Figs. 3 and 4, respectively. The TG curve consists of two-stage mass loss process. The endothermic peak appeared in both DTA and DSC curves is attributed to the dehydration reaction of the complex, while the exothermic one is attributed to the decomposition of the dehydrated complex.
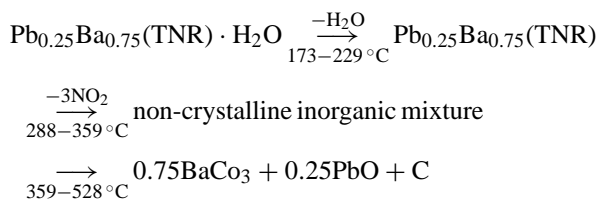
Table 3
Calculated values of the kinetic parameters for the dehydration and the decomposition reactions of the complex in flowing N_2 gas determined from the DSC curves at various heating rates

β (°C min^{-1})	T_e (°C)	E_o^a (kJ mol^{-1})	r_o^a	T_p (°C)	E_k^b (kJ mol^{-1})	$\log A_k^b$ (s^{-1})	r_k^b	E_o^a (kJ mol^{-1})	r_o^a	T_{e0} (°C)	T_b^c (°C)	T_{p0} (°C)	T_b^d (°C)
Dehydration reaction													
2.5	150.90	108.5	0.9995	176.28	105.7	9.71	0.9980	107.8	0.9983				
5.0	160.39			186.70									
10.0	170.47			196.54									
15.0	175.49			204.99									
Mean		(108.5 + 107.8)/2 = 108.2											
Exothermic decomposition reaction													
2.5	294.87	161.6	0.9872	310.66	165.3	12.18	0.9980	166.6	0.9982	273.83	290.16	293.16	310.14
5.0	306.15			321.72									
10.0	313.83			332.53									
15.0	325.66			341.63									
Mean		(161.6 + 166.6)/2 = 164.1											

β: heating rate; T_e: onset temperature in the DSC curve; T_p: maximum peak temperature; T_{e0}: the value (T_{e0}) of the onset temperature (T_e) corresponding to $\beta \to 0$ obtained by Eq. (7); T_b: critical temperature of thermal explosion; E: apparent activation energy; A: pre-exponential constant; r: linear correlation coefficient; subscript k: data obtained by Kissinger's method; subscript o: data obtained by Ozawa's method.

[a] Values of activation parameters calculated from the relationship of $\log \beta_i$ vs. $1/T_{ei}$ or $1/T_{pi}$.
[b] Values of activation parameters calculated from the relationship of $\ln(\beta_i/T_{pi}^2)$ vs. $1/T_{pi}$.
[c] The value of T_b obtained from Eq. (8) using the data of E_o and T_{e0}.
[d] The value of T_b obtained from Eq. (8) using the data of E_o and T_{p0}.

Table 4

Calculated values of the kinetic parameters for the major exothermic decomposition reaction of the complex under static air conditions determined from the DSC curves at various heating rates

β (°C min^{-1})	T_p (°C)	T_{p0} (°C)	Kissinger method			Ozawa method		T_b (°C)
			E_k (kJ mol^{-1})	$\log A_k$ (s^{-1})	r_k	E_o (kJ mol^{-1})	r_o	
2.0539	305.25	292.62	168.10	15.25	0.9990	169.30	0.9991	309.28
5.1597	318.75							
10.635	331.00							
21.007	344.00							

3.3. Analysis of kinetic data

In order to obtain the kinetic parameters [apparent activation energy (E_a) and pre-exponential constant (A)] of the dehydration reaction and the exothermic decomposition reaction for the complex, two multiple heating methods (Kissinger's method [5] and Ozawa's method [6]) were employed. From the original data in Tables 3 and 4, the values of E_k, A_k and r_k of the dehydration reaction obtained by Kissing's method are determined to be 105.7 kJ mol^{-1}, $10^{9.71}$ s^{-1}, 0.9980, respectively. The values of E_o and r_o obtained by Ozawa's method are 107.8 kJ mol^{-1} and 0.9983, respectively. For the exothermic decomposition reaction, E_k is determined to be 165.3 kJ mol^{-1} and A is $10^{12.18}$ s^{-1}. The value of r_k is 0.9980. The values of E_o and r_o are 166.6 kJ mol^{-1} and 0.9982, respectively. These values of E_a and A approach the values of E_a and A for the major exothermic decomposition of the complex in Table 4. It can be seen from Table 3 that the value of E_o obtained from the relationship of $\ln\beta$ versus T_e^{-1} is in good agreement with the calculated value obtained from the relationship of $\ln\beta$ versus T_p^{-1}, indicating that the value of E_o of 108.2 kJ mol^{-1} for the dehydration reaction and the value of E_o of 164.1 kJ mol^{-1} for the exothermic decomposition reaction are acceptable.

The integral equation (1) [7], differential equations (2) and (3) [8,9] are cited to obtain the values of E_a, A and the most probable kinetic model function [$f(\alpha)$] from a single non-isothermal DSC curve:

$$\ln\left[\frac{G(\alpha)}{T - T_0}\right] = \ln\left(\frac{A}{\beta}\right) - \frac{E_a}{RT} \tag{1}$$

$$\ln\left[\frac{d\alpha/dt}{f(\alpha)}\right] = \ln A - \frac{E_a}{RT} \tag{2}$$

$$\ln\left[\frac{d\alpha/dT}{f(\alpha)[E_\alpha(T - T_0)/RT^2 + 1]}\right] = \ln\left(\frac{A}{\beta}\right) - \frac{E_a}{RT} \tag{3}$$

where $f(\alpha)$ and $G(\alpha)$ are the differential and integral model functions, respectively, T_0 the initial point at which DSC curve deviates from the baseline, R the gas constant, α the conversion degree ($\alpha = H_t/H_0$), H_0 is the total heat effect corresponding to the global area under the DSC curve, H_t the reaction heat at a certain time (corresponding to the partial area under the DSC curve), T the temperature at time t, β the

Table 5

Kinetic model functions used for the present analysis

Function number	Function form	
	Integral form, $G(\alpha)$	Differential form, $f(\alpha)$
1	α^2	$\frac{1}{2}\alpha^{-1}$
2	$\alpha + (1 - \alpha)\ln(1 - \alpha)$	$[-\ln(1 - \alpha)]^{-1}$
3	$[1 - (1 - \alpha)^{1/2}]^{1/2}$	$4(1 - \alpha)^{1/2}[1 - (1 - \alpha)^{1/2}]^{1/2}$
4	$[1 - (1 - \alpha)^{1/2}]^2$	$(1 - \alpha)^{1/2}[1 - (1 - \alpha)^{1/2}]^{-1}$
5	$[1 - (1 - \alpha)^{1/3}]^{1/2}$	$6(1 - \alpha)^{2/3}[1 - (1 - \alpha)^{1/3}]^{1/2}$
6	$[1 - (1 - \alpha)^{1/3}]^2$	$\frac{3}{2}(1 - \alpha)^{2/3}[1 - (1 - \alpha)^{1/3}]^{-1}$
7	$1 - \frac{2}{3}\alpha - (1 - \alpha)^{2/3}$	$\frac{3}{2}[(1 - \alpha)^{-1/3} - 1]^{-1}$
8	$[(1 + \alpha)^{1/3} - 1]^2$	$\frac{3}{2}(1 + \alpha)^{2/3}[(1 + \alpha)^{1/3} - 1]^{-1}$
9	$[(1 - \alpha)^{-1/3} - 1]^2$	$\frac{3}{2}(1 - \alpha)^{4/3}[(1 - \alpha)^{-1/3} - 1]^{-1}$
10	$[-\ln(1 - \alpha)]^{1/4}$	$4(1 - \alpha)[-\ln(1 - \alpha)]^{3/4}$
11	$[-\ln(1 - \alpha)]^{\frac{1}{3}}$	$3(1 - \alpha)[-\ln(1 - \alpha)]^{2/3}$
12	$[-\ln(1 - \alpha)]^{2/5}$	$\frac{5}{2}(1 - \alpha)[-\ln(1 - \alpha)]^{3/5}$
13	$[-\ln(1 - \alpha)]^{1/2}$	$2(1 - \alpha)[-\ln(1 - \alpha)]^{1/2}$
14	$[-\ln(1 - \alpha)]^{2/3}$	$\frac{3}{2}(1 - \alpha)[-\ln(1 - \alpha)]^{1/3}$
15	$[-\ln(1 - \alpha)]^{3/4}$	$\frac{3}{4}(1 - \alpha)[-\ln(1 - \alpha)]^{1/4}$
16	$-\ln(1 - \alpha)$	$1 - \alpha$
17	$[-\ln(1 - \alpha)]^{3/2}$	$\frac{2}{3}(1 - \alpha)[-\ln(1 - \alpha)]^{-1/2}$
18	$[-\ln(1 - \alpha)]^2$	$\frac{1}{2}(1 - \alpha)[-\ln(1 - \alpha)]^{-1}$
19	$[-\ln(1 - \alpha)]^3$	$\frac{1}{3}(1 - \alpha)[-\ln(1 - \alpha)]^{-2}$
20	$[-\ln(1 - \alpha)]^4$	$\frac{1}{4}(1 - \alpha)[-\ln(1 - \alpha)]^{-3}$
21	$\ln\left[\frac{\alpha}{1 - \alpha}\right]$	$\alpha(1 - \alpha)$
22	$\alpha^{1/4}$	$4\alpha^{3/4}$
23	$\alpha^{1/3}$	$3\alpha^{2/3}$
24	$\alpha^{1/2}$	$2\alpha^{1/2}$
25	$1 - (1 - \alpha)^{1/1} = \alpha$	1
26	$\alpha^{3/2}$	$\frac{2}{3}\alpha^{-1/2}$
27	α^2	$\frac{1}{2}\alpha^{-1}$
28	$1 - (1 - \alpha)^{1/4}$	$4(1 - \alpha)^{3/4}$
29	$1 - (1 - \alpha)^{1/3}$	$3(1 - \alpha)^{2/3}$
30	$3[1 - (1 - \alpha)^{1/3}]$	$(1 - \alpha)^{2/3}$
31	$1 - (1 - \alpha)^{1/2}$	$2(1 - \alpha)^{1/2}$
32	$2[1 - (1 - \alpha)^{1/2}]$	$(1 - \alpha)^{1/2}$
33	$1 - (1 - \alpha)^2$	$\frac{1}{2}(1 - \alpha)^{-1}$
34	$1 - (1 - \alpha)^3$	$\frac{1}{3}(1 - \alpha)^{-2}$
35	$1 - (1 - \alpha)^4$	$\frac{1}{4}(1 - \alpha)^{-3}$
36	$(1 - \alpha)^{-1}$	$(1 - \alpha)^2$
37	$(1 - \alpha)^{-1} - 1$	$(1 - \alpha)^2$
38	$(1 - \alpha)^{-1/2}$	$2(1 - \alpha)^{3/2}$
39	$\ln\alpha$	α
40	$\ln\alpha^2$	$\frac{1}{2}\alpha$
41	$(1 - \alpha)^{-2}$	$\frac{1}{2}(1 - \alpha)^3$

Table 6
Basic data of the dehydration process of $Pb_{0.25}Ba_{0.75}(TNR)\cdot H_2O$ determined by DSC

Data point	T_i (K)	α_i	$(dH/dt)_i$ $(mJ\,s^{-1})$	$(d\alpha/dt)_i$ $(\times 10^4\,s^{-1})$	$(d\alpha/dT)_i$ $(\times 10^3\,K^{-1})$
1	425.65	0.0009	0.0063	0.6470	0.7767
2	428.15	0.0047	0.0146	1.4999	1.800
3	430.65	0.0116	0.0250	2.568	3.082
4	433.15	0.0222	0.0368	3.779	4.537
5	435.65	0.0379	0.0521	5.351	6.423
6	438.15	0.0594	0.0737	7.569	9.086
7	440.65	0.0891	0.1010	10.37	12.45
8	443.15	0.1275	0.1330	13.66	16.40
9	445.65	0.1777	0.1676	17.21	20.66
10	448.15	0.2385	0.2019	20.74	24.89
11	450.65	0.3101	0.2313	23.75	28.52
12	453.15	0.3902	0.2588	26.58	31.91
13	455.65	0.4784	0.2805	28.81	34.58
14	458.15	0.5722	0.2945	30.24	36.31
15	460.15	0.6690	0.2966	30.46	36.57
16	463.15	0.7652	0.2874	29.52	35.43
17	465.15	0.8551	0.2542	26.11	31.34
18	468.15	0.9308	0.1895	19.46	23.36
19	470.65	0.9800	0.0819	8.411	10.10
20	473.15	0.9971	0.0056	0.5751	0.6904

$T_0 = 423.15\,K$; $H_0 = 97.37\,mJ$; $\beta = 5\,K\,min^{-1}$.

heating rate and the value of $d\alpha/dT$ can be expressed as

$$\frac{d\alpha}{dT} = \frac{1}{H_0\beta}\frac{dH}{dt} = \frac{1}{\beta}\frac{d\alpha}{dt} \qquad (4)$$

Forty-one types of kinetic model function [10] in Table 5 and the data in Table 6 are put into Eqs. (1)–(3) for calculation. The values of E_a, A, r, standard mean square deviation (Q) and believable factor (d) (where $d = Q(1 - r)$ are obtained by the linear least-squares and iterative methods [7]. The results are listed in Tables 7 and 8. Comparing the kinetic parameters from three methods, we selected the probable kinetic model function number 15 whose values of E_a and $\log A$ are very close to each other with the better values of r, Q and d, indicating that the reaction mechanism of the dehydration process of the title complex is classified as nucleation and growth, and the mechanism function is the Avrami–Erofeev equation with $n = 3/4$. The calculated values of the kinetic parameters of the dehydration reaction and its probable kinetic model function obtained by the method of logical choice [7] are listed in Table 9. The values of E_a, A and the most probable kinetic model function obtained from an analysis of the original data in Table 10 are also summarized in

Table 7
Results of analysis of the dehydration process data of $Pb_{0.25}Ba_{0.75}(TNR)\cdot H_2O$ by integral (Eq. (1)) and differential (Eq. (2)) methods

Function number	Integral method					Differential method				
	E $(kJ\,mol^{-1})$	$\log A$ (s^{-1})	r	Q	d	E $(kJ\,mol^{-1})$	$\log A$ (s^{-1})	r	Q	d
1	334.40	33.05	0.9402	21.733	1.2997	277.54	28.72	0.8200	55.552	9.9966
2	357.55	35.53	0.9543	18.584	0.8502	326.35	34.27	0.8921	40.045	4.3638
3	28.73	−ve	0.9938	0.0153	0.0000	19.98	−ve	0.3430	4.4334	2.9126
4	374.59	37.27	0.9636	16.007	0.5832	365.85	38.68	0.9378	27.149	1.6880
5	32.94	−ve	0.9907	0.0030	0.0000	38.50	1.57	0.6859	2.4710	0.7762
6	391.46	38.94	0.9710	13.767	0.3995	397.01	42.06	0.9600	19.877	0.7959
7	368.31	36.17	0.9603	16.962	0.6738	351.54	36.62	0.9232	31.717	2.4362
8	314.16	29.65	0.9288	23.271	1.6573	248.53	24.26	0.7818	58.196	12.701
9	482.40	49.81	0.9870	9.1114	0.1181	533.43	58.37	0.9910	7.7179	0.0697
10	−ve	−ve	0.7700	0.4806	0.1106	9.01	−ve	0.2960	1.2518	0.8812
11	−ve	−ve	0.0096	0.2835	0.2808	30.62	0.94	0.7596	1.0174	0.2446
12	17.15	−ve	0.8469	0.1718	0.02630	47.90	2.98	0.8917	0.8759	0.0949
13	43.08	0.50	0.9856	0.0806	0.0012	73.83	6.03	0.9571	0.7402	0.0318
14	86.30	5.42	0.9940	0.1330	0.0008	117.05	11.07	0.9828	0.7181	0.0124
15	107.90	7.88	0.9927	0.2549	0.0019	138.65	13.58	0.9862	0.8028	0.0111
16	172.72	15.25	0.9888	1.0032	0.0112	203.48	21.08	0.9885	1.4394	0.0166
17	302.37	22.99	0.9848	4.2221	0.0643	333.12	36.00	0.9868	4.4351	0.0587
18	432.01	44.74	0.9828	9.7375	0.1672	462.76	50.88	0.9850	9.7272	0.1458
19	691.30	74.24	0.9810	27.658	0.5252	722.05	80.55	0.9828	27.201	0.4669
20	950.58	103.74	0.9801	54.764	1.0875	981.34	110.2	0.9816	53.860	0.9893
21	−ve	0.00	0.0000	–	–	−ve	−ve	0.1220	4.8039	4.2177
22	−ve	−ve	0.9359	0.2415	0.0155	−ve	−ve	0.7020	12.562	3.7432
23	−ve	−ve	0.9173	0.00751	0.0062	−ve	−ve	0.6098	13.419	5.2355
24	18.68	−ve	0.9159	0.0992	0.0083	−ve	−ve	0.3497	15.491	10.074
25	123.92	9.40	0.9394	3.0272	0.1834	67.06	4.27	0.4619	24.561	13.217
26	229.16	21.23	0.9400	10.240	0.6141	172.30	16.77	0.7327	37.914	10.133
27	334.40	33.05	0.9402	21.173	1.2997	277.54	28.72	0.8201	55.552	9.9966
28	157.07	12.77	0.9815	1.3882	0.0256	169.37	16.40	0.9567	3.9348	0.1704
29	152.45	12.35	0.9779	1.5711	0.0347	158.01	15.17	0.9357	5.2533	0.3377
30	152.45	12.82	0.9779	1.5711	0.0347	158.01	15.64	0.9357	5.2533	0.3377
31	144.01	11.51	0.9695	1.9610	0.0598	135.27	12.62	0.8710	8.6202	1.1120
32	144.01	11.81	0.9695	1.9610	0.0598	135.27	12.93	0.8710	8.6202	1.1120
33	97.51	6.53	0.8754	4.2926	0.5349	−ve	−ve	0.2815	82.722	59.434

Table 7 (*Continued*)

Function number	Integral method					Differential method				
	E (kJ mol^{-1})	log A (s^{-1})	r	Q	d	E (kJ mol^{-1})	log A (s^{-1})	r	Q	d
33	97.51	6.53	0.8754	4.2926	0.5349	−ve	−ve	0.2815	82.722	59.434
34	80.09	4.60	0.8134	4.8594	0.9070	−ve	−ve	0.5126	175.92	85.751
35	67.28	3.17	0.7536	5.1009	1.2571	−ve	−ve	0.6025	304.16	120.90
36	49.85	2.06	0.3575	25.107	16.131	339.89	37.39	0.9631	13.357	0.4928
37	260.33	25.71	0.9560	9.4578	0.4165	339.89	37.39	0.9631	13.357	0.4928
38	−ve	−ve	0.2304	8.9008	6.8502	271.68	28.93	0.9865	3.0185	0.0408
39	−ve	0.00	0.0000	–	–	−ve	−ve	0.8602	10.704	1.4964
40	−ve	0.00	0.0000	–	–	−ve	−ve	0.8602	10.704	1.4964
41	186.26	18.37	0.6165	83.799	32.139	476.30	54.00	0.9207	60.315	4.7801

Table 9. These values of E_a and A obtained from a single non-isothermal DSC curve are in good agreement with the calculated values obtained by Kissinger's method and Ozawa's method.

Substituting $f(\alpha)$ with $(3/4)(1 - \alpha)[-\ln(1 - \alpha)]^{1/4}$, E_a with 111.12 kJ mol^{-1}, and A with $10^{9.55}$ s^{-1} in Eq. (5)

$$\frac{d\alpha}{dT} = \frac{A}{\beta} f(\alpha) \exp\left(-\frac{E_a}{RT}\right) \tag{5}$$

Table 8

Results of analysis of the dehydration process data of Pb$_{0.25}$Ba$_{0.75}$(TNR)·H$_2$O by differential (Eq. (3)) method

Function number	E_a (kJ mol^{-1})	log A (s^{-1})	r	Q	d
1	225.05	22.01	0.7745	49.08	10.92
2	270.97	27.16	0.8718	34.31	4.398
3	11.33	−ve	0.2039	4.379	3.486
4	308.55	31.31	0.9310	21.65	1.493
5	23.04	−ve	0.4975	2.390	1.201
6	338.441	34.51	0.9587	14.94	0.6175
7	294.90	29.34	0.9123	25.96	2.278
8	198.11	17.83	0.7266	51.97	14.21
9	470.58	50.20	0.9908	6.140	0.0567
10	4.93	−ve	0.1667	1.259	3.486
11	17.92	−ve	0.5585	1.049	0.4633
12	29.39	0.68	0.7621	0.9229	0.2196
13	48.04	2.80	0.9016	0.7866	0.0774
14	82.10	6.67	0.9675	0.6808	0.0221
15	100.15	8.72	0.9778	0.6829	0.0152
16	157.00	15.18	0.9876	0.9252	0.0115
17	277.38	28.85	0.9886	2.640	0.0301
18	401.87	43.00	0.9872	6.243	0.0799
19	655.59	71.84	0.9848	19.71	0.2983
20	911.93	101.0	0.9834	41.94	0.6966
21	−ve	−ve	0.0634	4.795	4.491
22	−ve	–	–	–	–
23	−ve	–	–	–	–
24	−ve	–	–	–	–
25	43.02	1.27	0.3223	23.64	16.02
26	129.24	11.32	0.6467	34.40	12.15
27	225.05	22.01	0.7745	49.08	10.92
28	126.67	10.99	0.9427	2.973	0.1702
29	116.75	9.95	0.9101	4.186	0.3764
30	116.75	10.43	0.9101	4.186	0.3764
31	97.29	7.83	0.8087	7.416	1.419
32	97.29	8.14	0.8087	7.416	1.419
33	−ve	–	–	–	–
34	−ve	–	–	–	–
35	−ve	–	–	–	–
36	283.81	30.19	0.9390	16.01	0.9766
37	283.81	30.19	0.9390	16.01	0.9766
38	219.58	22.28	0.9740	3.866	0.1006
39	−ve	–	–	–	–
40	−ve	–	–	–	–
41	414.99	46.06	0.8894	67.36	7.449

Table 9
Calculated values of kinetic parameters of dehydration reaction for the complex

β (°C)	$G(\alpha)$	$f(\alpha)$	Eq. (1)		Eq. (2)		Eq. (3)	
			E_a (kJ mol^{-1})	$\log A$ (s^{-1})	E_a (kJ mol^{-1})	$\log A$ (s^{-1})	E_a (kJ mol^{-1})	$\log A$ (s^{-1})
5	$[-\ln(1-\alpha)]^{3/4}$	$\frac{3}{4}(1-\alpha)[-\ln(1-\alpha)]^{1/4}$	107.90	7.88	138.65	13.58	100.15	8.72
15	$[-\ln(1-\alpha)]^{3/4}$	$\frac{3}{4}(1-\alpha)[-\ln(1-\alpha)]^{1/4}$	110.37	8.06	118.96	11.36	90.72	7.72
Mean			111.12 ($\log A$ (s^{-1}) = 9.55)					

Table 10
Basic data of the dehydration process of $Pb_{0.25}Ba_{0.75}(TNR) \cdot H_2O$ determined by DSC

Data point	T_i (K)	α_i	$(dH/dt)_i$ (mJ s^{-1})	$(d\alpha/dt)_i$ ($\times 10^4$ s^{-1})	$(d\alpha/dT)_i$ ($\times 10^3$ K^{-1})
1	430.65	0.0005	0.0195	2.566	1.026
2	433.15	0.0029	0.0295	3.882	1.553
3	433.65	0.0058	0.0415	5.461	2.184
4	438.15	0.0116	0.0555	7.303	2.921
5	440.65	0.0181	0.0700	9.211	3.684
6	443.15	0.0285	0.0875	11.51	4.605
7	445.65	0.0395	0.1060	13.95	5.579
8	448.15	0.0552	0.1305	17.17	6.868
9	450.65	0.0726	0.1585	20.86	8.342
10	453.15	0.0961	0.1915	25.20	10.08
11	455.65	0.1234	0.2319	30.51	12.21
12	458.15	0.1572	0.2829	37.22	14.89
13	460.65	0.1989	0.3430	45.13	18.05
14	463.15	0.2500	0.4090	53.82	21.53
15	465.65	0.3088	0.4789	63.01	25.21
16	468.15	0.3751	0.5436	71.53	28.61
17	470.65	0.4503	0.5987	78.78	31.51
18	473.15	0.5326	0.6405	84.28	33.71
19	475.65	0.6193	0.6623	87.14	34.86
20	478.15	0.7079	0.6680	87.89	35.16
21	480.65	0.7954	0.6399	84.20	33.68
22	483.15	0.8763	0.5631	74.09	29.64
23	485.65	0.9421	0.4023	52.93	21.17
24	488.15	0.9809	0.1755	23.09	9.237
25	490.65	0.9961	0.0385	5.066	2.026
26	493.15	0.9993	0.0065	0.8553	0.3421

$T_0 = 423.15$ K; $H_0 = 76.00$ mJ; $\beta = 15$ K min^{-1}.

we can establish the kinetic equation of the dehydration process of the title complex as follows:

$$\frac{d\alpha}{dT} = \frac{10^{9.43}}{\beta}(1-\alpha)[-\ln(1-\alpha)]^{1/4} e^{-1.337 \times 10^4/T} \quad (6)$$

Under the condition of flowing N$_2$ gas, the values (T_{e0} and T_{p0}) of the onset temperature (T_e) and the peak temperature (T_p) corresponding to $\beta \to 0$ obtained by Eq. (7) taken from Ref. [10] using the data of T_e, T_p and β in Table 1 are 273.83 and 293.16 °C, respectively:

$$T_{(e\,or\,p)_i} = T_{e0\,or\,p0} + b\beta_i + c\beta_i^2 + d\beta_i^3, \quad i = 1, 2, 3 \quad (7)$$

where b, c and d are the coefficients.

The values of the critical temperature of thermal explosion (T_b) obtained from Eq. (8) taken from Ref. [10] using the above-mentioned values of T_{e0} and T_{p0}, and the value of E_o

in Table 3 are 290.16 and 310.14 °C, respectively:

$$T_b = \frac{E_o - \sqrt{E_o^2 - 4E_o R T_{e0\,or\,p0}}}{2R} \quad (8)$$

where R is the gas constant (8.314 J mol^{-1} K^{-1}) and E_o the value of E obtained by Ozawa's method.

Under static air conditions, the values of T_{p0} and T_b obtained by Eqs. (7) and (8) using the values of T_{p0}, β and E_o in Table 4 are 292.62 and 309.28 °C, respectively. These values approach the calculated values under the condition of flowing N$_2$ gas, indicating that under our experimental conditions, the atmosphere have no effect on the values of T_{p0} and T_b of the complex.

4. Conclusions

The mechanism of the thermal decomposition reaction of the complex under static air conditions could be described by

the scheme shown in text. The most probable kinetic model function in integral form, apparent activation energy and pre-exponential constant for the dehydration reaction in flowing N_2 gas are $[-\ln(1-\alpha)]^{3/4}$, 111.12 kJ mol^{-1} and $10^{9.55}$ s^{-1}, respectively. The kinetic equation of this process can be expressed as

$$\frac{d\alpha}{dT} = \frac{10^{9.43}}{\beta}(1-\alpha)[-\ln(1-\alpha)]^{1/4}\,e^{-1.337\times10^4/T}$$

The apparent activation energy and pre-exponential constant of the major exothermic decomposition reaction of the complex in static air conditions are 168.10 kJ mol^{-1} and $10^{15.25}$ s^{-1}, respectively. Its critical temperature of thermal explosion is about 310 °C.

References

[1] Z.Y. Du, Acta Armamentarii 3 (1982) 31.
[2] R.Z. Hu, Z.Y. Du, C.Y. Wu, J.S. Wang, Y.J. Liang, J.M. Li, J. Inorg. Chem. 3 (4) (1987) 121 (in Chinese).
[3] Z.J. Chen, R.R. Ge, Explosive Mater. 30 (3) (2001) 16.
[4] Z.Y. Du, R.Z. Hu, J.S. Wang, C.Y. Wu, Y.J. Liang, in: D. Jing (Ed.), Proceeding of the International Symposium on Pyrotechnics and Explosives, #####, China Academic Publishers, Beijing, 1987, pp. 376–381.
[5] H.E. Kissinger, Anal. Chem. 29 (1957) 1702.
[6] T. Ozawa, Bull. Chem. Soc. Jpn. 38 (1965) 1881.
[7] R.Z. Hu, Z.Q. Yang, Y.J. Ling, Thermochim. Acta 123 (1988) 135.
[8] J.H. Sharp, S.A. Wendworth, Anal. Chem. 41 (14) (1969) 2060.
[9] T.P. Bagchi, K.P. Sen, Thermochim. Acta 51 (2–3) (1981) 175.
[10] T.L. Zhang, R.Z. Hu, Y. Xie, F.P. Li, Thermochim. Acta 244 (1994) 171.